# Chapter 8
# Delayed Differentiation Makes Many Models Compatible with Data for CD8$^+$ T Cell Differentiation


**Aridaman Pandit and Rob J. de Boer**

## 8.1 Introduction

The adaptive immune system is characterized by its ability to mount specific responses against many invading pathogens and to form long-lived memory to each of these pathogens and rapidly respond when the pathogen reinfects the host. This ability to form long-lived memory forms the basis of vaccination. CD8$^+$ T cells (or cytotoxic T cells) form an integral part of the adaptive immune system and are known to mount a cytotoxic response especially against intracellular pathogens like viruses. CD8$^+$ T cells respond by recognizing a cognate peptide on a MHC with their T cell receptor (TCR). Upon activation, naïve CD8$^+$ T cells undergo rapid proliferation producing $10^5$ progenies [1]. In mice single epitopes from a virus activate 100 to 1000 naïve CD8$^+$ T cells [2, 3], which expand vigorously and together form a total immune response of more than $10^7$ cells. After this peak, the CD8$^+$ T cell population undergoes a contraction phase leaving behind about 5% of the antigen-specific CD8$^+$ T cells. These memory CD8$^+$ T cells are longer-lived and can mount a rapid response in case of reinfection. For a given infection, the magnitude and expansion and contraction pattern of CD8$^+$ T cell response have been shown to be highly reproducible [4]. Studies have shown that individual naïve CD8$^+$ T cells can produce both memory and effector cells [1]. Single-cell

A. Pandit (✉)
Center for Translation Immunology, Utrecht Medical Center Utrecht (UMCU), Utrecht, The Netherlands

Department of Rheumatology and Clinical Immunology, University Medical Center Utrecht (UMCU), Utrecht, The Netherlands
e-mail: A.Pandit@umcutrecht.nl

R. J. de Boer
Theoretical Biology and Bioinformatics, Utrecht University, Utrecht, The Netherlands
e-mail: r.j.deboer@uu.nl



C. Molina-París, G. Lythe (eds.), *Mathematical, Computational and Experimental T Cell Immunology*, https://doi.org/10.1007/978-3-030-57204-4_8

tracing studies have shown that fate of individual naïve $CD8^+$ T cell varies, which is probably governed by several biological and stochastic factors [4, 5]. The fate and memory potential of individual $CD8^+$ T cells is an active field of study.

Several models for $CD8^+$ T cell differentiation have been proposed [6–8]. In the 'linear differentiation' model, effector $CD8^+$ T cells produced during the expansion phase either die or form memory $CD8^+$ T cells during the contraction phase. In the 'progressive differentiation' model, the strength of stimulation determines the fate of individual $CD8^+$ T cells [6, 7]. Excessive stimulation may lead to terminally differentiated effector cells, while weak stimulation may lead to memory cells [6, 7]. In the 'asymmetric division' model, one daughter cell acquires memory potential and the other daughter cell acquires effector potential, during the first division of a progenitor cell [9]. Several other models have been proposed, highlighting the roles of strength and nature of stimulation, niches and timing of differentiation, in determining the fate of individual naïve $CD8^+$ T cell [6–8].

Two single-cell tracing studies [4, 5] showed that fate of individual naïve $CD8^+$ T cell is disparate. These studies demonstrated that the number of daughter cells produced from individual naïve $CD8^+$ T cells bearing the same TCR is extremely variable. In both studies, the expression of surface markers CD62L and CD27 was measured and correlated with the number of progenies produced by individual naïve $CD8^+$ T cells (i.e. a family of naïve T cells). CD62L marker expression negatively correlated with family sizes, whereas CD27 marker expression was not significantly correlated [4, 5]. This agrees with the fact that CD62L expression decreases with cellular division [10].

Buchholz et al. [5] defined $CD62L^+CD27^+$ as central memory precursors ($CM$), $CD62L^-CD27^+$ as effector memory precursors ($EM$) and $CD62L^-CD27^-$ as effector ($F$) $CD8^+$ T cells. Using the heterogeneity in marker distributions for different naïve $CD8^+$ T cell families, they showed that a linear differentiation model from naïve to $CM$ to $EM$ to $F$ cells describes their single-cell tracing data the best. Buchholz et al. [5] modelled the proliferation and differentiation dynamics as a standard Markov process and interestingly used both the first and the second moments to discriminate between different models of $CD8^+$ T cell differentiation. Although the approach used by Buchholz et al. [5] robustly showed that 'memory first' models better fit their data, all models tested assumed that the rate of cellular differentiation and proliferation reflects an exponential process. However, several studies have shown that the division and differentiation of T cells is not exponential and is better described by a delayed distribution, like a gamma or a lognormal distribution [11–14]. Here we tested how incorporation of a delay during differentiation affects the inference that 'memory first' models describe the data best. In a companion paper, we have studied the effect of non-exponential division [8].

## 8.2 Models and Results

We used ordinary differential equations to model the delayed differentiation of CD8$^+$ T cells by extending the model of Buchholz et al. [5], who suggested that naïve CD8$^+$ T cells first differentiate into central memory precursors ($CM$), followed by differentiation into effector memory precursors ($EM$) and subsequently into effectors ($F$). We will call this original model the 'linear basic' model. Importantly, the *linear basic* model assumes simple exponential differentiation kinetics for different CD8$^+$ T cell subsets. We will first show that variants of the *linear* model, which allow for delayed differentiation of CD8$^+$ T cell subsets, have population dynamics that is comparable to the *linear basic* model. Subsequently, we test whether alternative models with delayed differentiation dynamics can also describe the CD8$^+$ T cell subset dynamics with similar accuracy. We further performed Gillespie simulations to test whether the predicted variance of the alternative models is comparable to that of the *linear basic* model.

### *8.2.1 Linear Models*

To create an accurate data set, we simply ran the best model proposed by Buchholz et al. [5]. In this model, naïve CD8$^+$ T cells ($N$) differentiate into $CM$ CD8$^+$ T cells at a rate $n$ (Eq. 8.1). $CM$ CD8$^+$ T cells proliferate at a rate $p_{CM}$ and differentiate into $EM$ CD8$^+$ T cells at a rate $d_{CM}$ (Eq. 8.2). $EM$ CD8$^+$ T cells proliferate at a rate $p_{EM}$ and differentiate into effector CD8$^+$ T cells at a rate $d_{EM}$ (Eq. 8.3). Effector CD8$^+$ T cells further proliferate at a rate $p_F$ (Eq. 8.4).

$$\frac{dN}{dt} = -n \cdot N \tag{8.1}$$

$$\frac{dCM}{dt} = n \cdot N + p_{CM} \cdot CM - d_{CM} \cdot CM \tag{8.2}$$

$$\frac{dEM}{dt} = d_{CM} \cdot CM + p_{EM} \cdot EM - d_{EM} \cdot EM \tag{8.3}$$

$$\frac{dF}{dt} = d_{EM} \cdot EM + p_F \cdot F \tag{8.4}$$

To depict the population dynamics of a typical family, we set $N(0) = 1$, $CM(0) = EM(0) = F(0) = 0$ and observe that the first $CM$ CD8$^+$ T cells appear around day 1 (Fig. 8.1a, b) and that this population keeps on increasing (because $p_{CM} > d_{CM}$; see Table 8.1 for parameter values). $EM$ and $F$ CD8$^+$ T cells appear at around day 2 and day 3, respectively, and their populations also increase over time. However, since the growth in $CM$ population is slower compared to that of the $EM$ and $F$ populations, the fraction of the $CM$ population declines over time (Fig. 8.1b). To

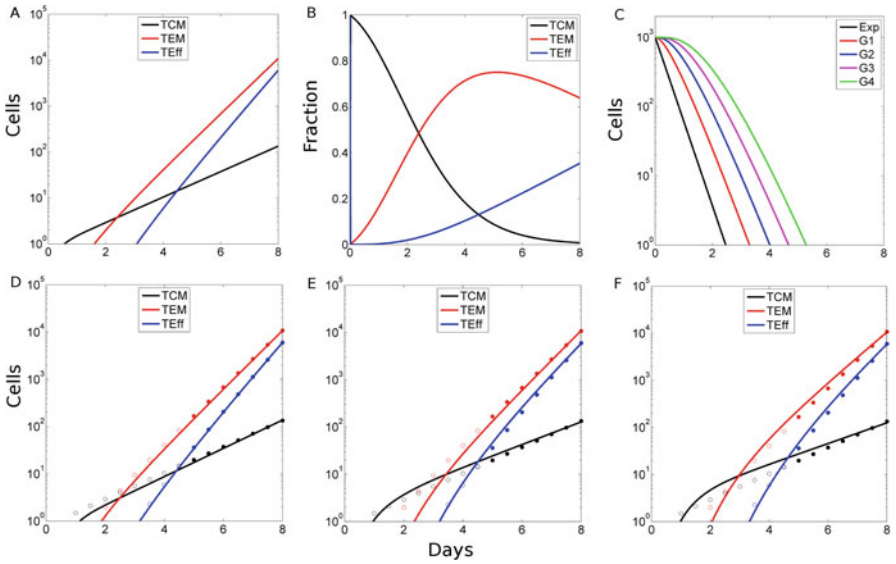


**Fig. 8.1** Various *linear* models. Population dynamics (**a**) and relative fraction (**b**) of different CD8$^+$ T cell subsets obtained from the *linear basic* model using the original parameter values given in the first line of Table 8.1. Panel (**c**) depicts the effect of delaying the recruitment of naive cells into the first phenotype capable of cell division (TCM). Starting with $N = 10^3$ cells, the loss of naive cells as described by equation (8.1) is shown for $K_N = 0$ (black: Exp) and $K_N = 1$ (red: G1) to $K_N = 4$ (green: G4). Panels (**d**) to (**f**) depict the population dynamics of alternate *linear* models with delayed differentiation: (**d**) *linear N3*: $K_N = 3, K_M = 0$, (**e**) *linear A3*: $K_N = K_M = 3$ and (**f**) *linear A4*: $K_N = K_M = 4$. Population means predicted by the best fit delayed differentiation models are shown for different T cell subsets: central memory (TCM; black lines), effector memory (TEM; red lines) and effector (**f**; blue lines) cells. The models were fitted to the population means of days 5–8 (shown as filled circles) obtained from the *linear basic* model given in Fig. 8.1a. The population means of days 0–4 of the original model were not used for fitting the parameters and are shown as open circles. For the best fit parameters, see Table 8.1

match the sampling times of the original paper [5], our alternative models were fitted to the 'data' at days 5 to 8 in Fig. 8.1.

In the *linear basic* model, the differentiation of $N$, $CM$ and $EM$ CD8$^+$ T cells was assumed to be an exponential process. However, several studies have shown that the differentiation of T cells is not exponential [11–14]. So, we were interested in the effect of delays in the model for differentiation of CD8$^+$ T cell subsets. In order to incorporate delays, while keeping the number of parameters constant, we developed transit models with $K$ compartments that approximate a gamma distribution for large values of $K$. Thus, we developed a set of models where each of the differentiation steps can be subdivided into one to several stages. In Eqs. 8.5–8.11, we subdivide each subpopulation into $k$ stages, where $k = 0, 1, \ldots, K_N$ for the recruitment of naive cells, and $k = 0, 1, \ldots, K_M$ for the memory T cells.

**Table 8.1** The original (line 1) and the best fit parameter values obtained for the *linear* models

| Model | $K_N$ | $K_M$ | $n$ | $d_{CM}$ | $d_{EM}$ | $p_{CM}$ | $p_{EM}$ | $p_F$ | $SSR$ |
|---|---|---|---|---|---|---|---|---|---|
| Linear basic | 0 | 0 | 2.800 | 0.192 | 0.039 | 0.830 | 1.420 | 1.590 | – |
| Linear N1 | 1 | 0 | 3.375 | 0.229 | 0.052 | 0.887 | 1.447 | 1.541 | 0.061 |
| Linear N2 | 2 | 0 | 3.850 | 0.393 | 0.061 | 1.067 | 1.398 | 1.463 | 0.075 |
| Linear N3 | 3 | 0 | 4.314 | 0.282 | 0.058 | 0.971 | 1.481 | 1.564 | 0.064 |
| Linear N4 | 4 | 0 | 4.688 | 0.388 | 0.029 | 1.091 | 1.428 | 1.726 | 0.088 |
| Linear A1 | 1 | 1 | 3.379 | 0.610 | 0.641 | 1.210 | 2.037 | 1.237 | 0.051 |
| Linear A2 | 2 | 2 | 3.865 | 1.200 | 2.525 | 1.764 | 3.825 | 0.361 | 0.234 |
| Linear A3 | 3 | 3 | 4.302 | 1.256 | 2.973 | 1.808 | 4.413 | 0.804 | 0.123 |
| Linear A4 | 4 | 4 | 4.722 | 2.598 | 2.383 | 3.105 | 3.598 | 1.130 | 0.214 |

$$\frac{dN_0}{dt} = -n \cdot N_0 \tag{8.5}$$

$$\frac{dN_k}{dt} = n \cdot N_{k-1} - n \cdot N_k, \quad \text{for} \quad k = 1, 2, \ldots, K_N \tag{8.6}$$

$$\frac{dCM_0}{dt} = n \cdot N_k + p_{CM} \cdot CM_0 - d_{CM} \cdot CM_0 \tag{8.7}$$

$$\frac{dCM_k}{dt} = d_{CM} \cdot CM_{k-1} - d_{CM} \cdot CM_k, \quad \text{for} \quad k = 1, 2, \ldots, K_M \tag{8.8}$$

$$\frac{dEM_0}{dt} = d_{CM} \cdot CM_k + p_{EM} \cdot EM_0 - d_{EM} \cdot EM_0 \tag{8.9}$$

$$\frac{dEM_k}{dt} = d_{EM} \cdot EM_{k-1} - d_{EM} \cdot EM_k, \quad \text{for} \quad k = 1, 2, \ldots, K_M \tag{8.10}$$

$$\frac{dF}{dt} = d_{EM} \cdot EM_k + p_F \cdot F \tag{8.11}$$

Our first version of this model is to only allow for stages in the differentiation of naïve CD8$^+$ T cells ($K_M = 0$), and we refer to these models as the *linear Nk* model, where $k$ reflects the number of stages. Hence the *linear N0* model is identical to the original model proposed by Buchholz et al. [5]. The *linear N4* model has four stages of naïve CD8$^+$ T cell differentiation in Eq. 8.6. In our second set of models, we allow all differentiation steps to be non-exponential. We call these the *linear Ak* models, where again the *linear A0* model is identical to the original model. All models were fitted to the data produced by running the original model, using the late time points at days 5 to 8 (filled circles in Fig. 8.2) to estimate parameters. Parameter estimates are provided in Table 8.1.

We could fit all *linear N1–4* and *linear A1–4* models to the *linear basic* model with a weighted sum of squared residuals (wSSR) value $< 0.25$. Figure 8.1d–f depicts three examples of delayed *linear* models (i.e. *linear N3*, *linear A3* and *linear A4*) to illustrate the quality of the fit. Even though the models were fitted to day 5–8 data only, the models predict population means comparable to the day 0–4 data.

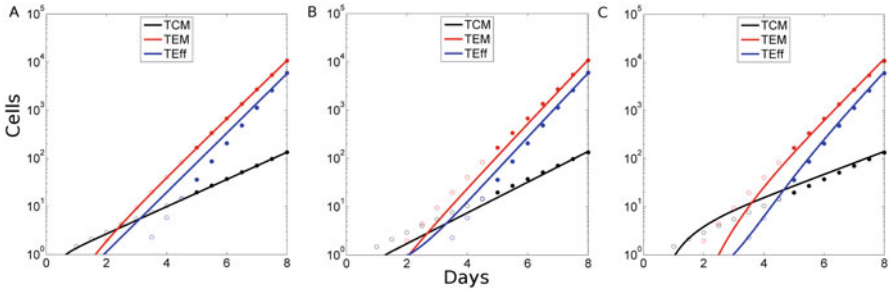


**Fig. 8.2** Population dynamics of different branching models: (**a**) *Fate basic*, (**b**) *Branching basic* and (**c**) *Fate A4*. Population means predicted by the branching models are shown for different T cell subsets: central memory (TCM; black lines), effector memory (TEM; red lines) and effector (F; blue lines) cells. The models were fitted to the population means of days 5–8 (shown as filled circles) obtained from the *linear basic* model given in Fig. 8.1a. The population means of day 0–4 of the original model were not used for fitting the parameters and are shown as open circles. Parameter values given in Table 8.2

Interestingly, in all models with a delay in naïve differentiation only, the rate of proliferation increases with the stages of differentiation (as was described for the original model [5]). However, this pattern is absent from the *linear Ak* models where all differentiation steps are non-exponential. Thus, the original conclusion that the differentiation of naïve $CD8^+$ T cells progresses through slowly proliferating memory precursors towards rapidly proliferating effector cells [5] depends on the assumption that differentiation is an exponential process in the *linear basic* model.

### 8.2.2 Branching and Fate Models

Since the incorporation of delay during differentiation of $CD8^+$ T cells resulted in similarly good fits of the models, we decided to test whether alternate models can produce population dynamics similar to the *linear basic* model. We first developed a branching model where a fraction ($f$) of naïve $CD8^+$ T cells differentiates into effectors ($F$) and the remaining into $CM$ $CD8^+$ T cells. These models assume a division of labour, as a fraction of the naïve $CD8^+$ T cells differentiates directly into effector cells, while the remaining naïve cells differentiate into memory cells and follow the same linear differentiation pathway towards effector cells. Thus, replacing equations (8.7) and (8.11) with

$$\frac{dCM_0}{dt} = (1-f)\cdot n \cdot N_k + p_{CM}\cdot CM_0 - d_{CM}\cdot CM_0 \tag{8.12}$$

$$\frac{dF}{dt} = f\cdot n \cdot N_k + d_{EM}\cdot EM_k + p_F \cdot F \tag{8.13}$$

**Table 8.2** The best fit parameter values obtained for different *Branching* models

| Model[a] | $K_N$ | $K_M$ | $n$ | $d_{CM}$ | $d_{EM}$ | $p_{CM}$ | $p_{EM}$ | $p_F$ | $f$ | $SSR$ |
|---|---|---|---|---|---|---|---|---|---|---|
| Branching basic | 0 | 0 | 2.799 | 0.100 | 0.355 | 0.752 | 1.852 | 0.837 | 0.1 | 0.065 |
| Branching basic | 0 | 0 | 2.799 | 0.091 | 0.782 | 0.759 | 2.309 | 0.061 | 0.2 | 0.068 |
| Branching basic | 0 | 0 | 2.800 | 0.137 | 0.741 | 0.870 | 2.265 | 0.137 | 0.5 | 0.100 |
| Branching N1 | 1 | 0 | 3.375 | 0.124 | 0.319 | 0.797 | 1.827 | 0.920 | 0.1 | 0.131 |
| Branching N2 | 2 | 0 | 3.869 | 0.330 | 0.269 | 1.020 | 1.654 | 0.905 | 0.1 | 0.143 |
| Branching N3 | 3 | 0 | 4.313 | 0.545 | 0.381 | 1.334 | 1.788 | 0.708 | 0.5 | 0.189 |
| Branching N4 | 4 | 0 | 4.730 | 0.110 | 0.471 | 0.829 | 2.097 | 0.758 | 0.1 | 0.122 |
| Branching A1 | 1 | 1 | 3.374 | 0.618 | 1.634 | 1.319 | 3.099 | 0.433 | 0.5 | 0.101 |
| Branching A2 | 2 | 2 | 3.893 | 1.237 | 1.474 | 1.815 | 2.807 | 1.012 | 0.1 | 0.127 |
| Branching A3 | 3 | 3 | 4.307 | 0.871 | 3.922 | 1.462 | 5.567 | 0.666 | 0.1 | 0.164 |
| Branching A4 | 4 | 4 | 4.712 | 1.664 | 3.349 | 2.211 | 4.801 | 1.017 | 0.1 | 0.178 |
| Branching A4 | 4 | 4 | 4.725 | 1.931 | 5.734 | 2.567 | 7.159 | 0.180 | 0.5 | 0.145 |

[a]Note: some models exhibiting similar SSR values are not given in the table

respectively, we define our branching models. To keep the number of parameters constant, we fixed $f$ at either 0.1, 0.2 or 0.5.

In the first set of branching models, we allowed $EM$ cells to differentiate into effector CD8$^+$ T cells (i.e. $d_{EM} > 0$ in equation (8.13)), and we refer to these as the *Branching* models. We found good fits (SSR $\leq$ 0.1) for the *Branching basic* models, $K_N = K_M = 0$, for all three values of $f$ (Table 8.2). This indicates that the branching model where 50% of naïve CD8$^+$ T cells differentiate directly into effector cells can describe the population means of different CD8$^+$ T cell subsets as predicted by the original model (Fig. 8.2b). Subsequently, we incorporated delay during differentiation of different CD8$^+$ T cell subsets for the *Branching* model. For models with delay during differentiation, of either only naïve cells or all CD8$^+$ T cell subsets, we obtain good fits with a SSR $\leq$ 0.2 (Table 8.2).

We next developed models where the fate of the naïve CD8$^+$ T cells was defined before, or during, their activation. This means that a fraction of naïve cells differentiates into memory cells only, while the remainder differentiates directly into effector cells. This was implemented by setting $d_{EM} = 0$ in Eq. (8.13), and we refer to this as the *Fate* models. The fits of the *Fate* model were in general worse than those of the *Branching* model fits, with several models having their best fit SSR value $> 0.25$ (Table 8.3). The *Fate basic* model with $f = 0.5$ had a best fit with a high SSR value of 0.464 (Table 8.3 and Fig. 8.2a). Incorporating delays during differentiation allowed us to achieve somewhat better fits for the *Fate* models (Table 8.3 and Fig. 8.2c), but overall, we found that the *Branching* models outperformed the *Fate* models.

**Table 8.3** The best fit parameter values obtained for different *Fate* models

| Model[a] | $K_N$ | $K_M$ | $n$ | $d_{CM}$ | $p_{CM}$ | $p_{EM}$ | $p_F$ | $f$ | $SSR$ |
|---|---|---|---|---|---|---|---|---|---|
| Fate basic | 0 | 0 | 2.801 | 0.199 | 0.851 | 1.389 | 1.422 | 0.1 | 0.109 |
| Fate basic | 0 | 0 | 2.800 | 0.205 | 0.874 | 1.399 | 1.330 | 0.2 | 0.216 |
| Fate basic | 0 | 0 | 2.801 | 0.300 | 1.033 | 1.400 | 1.209 | 0.5 | 0.464 |
| Fate N1 | 1 | 0 | 3.375 | 0.263 | 0.936 | 1.385 | 1.462 | 0.1 | 0.141 |
| Fate N2 | 2 | 0 | 3.832 | 0.337 | 1.044 | 1.398 | 1.401 | 0.2 | 0.175 |
| Fate N3 | 3 | 0 | 4.310 | 0.686 | 1.390 | 1.283 | 1.525 | 0.1 | 0.202 |
| Fate N4 | 4 | 0 | 4.701 | 0.529 | 1.247 | 1.357 | 1.552 | 0.1 | 0.378 |
| Fate A1 | 1 | 1 | 3.379 | 1.298 | 1.896 | 1.249 | 1.462 | 0.1 | 0.123 |
| Fate A2 | 2 | 2 | 3.859 | 1.634 | 2.221 | 1.361 | 1.400 | 0.2 | 0.146 |
| Fate A3 | 3 | 3 | 4.333 | 2.257 | 2.799 | 1.363 | 1.522 | 0.1 | 0.161 |
| Fate A4 | 4 | 4 | 4.738 | 1.884 | 2.422 | 1.581 | 1.550 | 0.1 | 0.228 |
| Fate A4 | 4 | 4 | 4.734 | 2.320 | 2.948 | 1.578 | 1.322 | 0.5 | 0.300 |

[a]Note: some models exhibiting similar SSR values are not given in the table

### *8.2.3 Variations in Family Sizes*

Ideally, fitting various mathematical models to data should provide us sufficient information to discriminate between different biological hypotheses [15, 16]. Using data on population averages only, we have seen above that this fails to discriminate between a linear chain and a branching model. Importantly, Buchholz et al. [5] used variances and covariance of different T cell populations to discriminate between different models of $CD8^+$ T cell differentiation. To also study the stochasticity in different $CD8^+$ T cell subsets, we performed 10,000 Monte Carlo simulations for each model using the Gillespie algorithm [17, 18]. We compared the mean cell numbers and variances of $CM$, $EM$ and $F$ $CD8^+$ T cells predicted by Gillespie simulations for different *linear* models (Fig. 8.3). Since we used the parameters obtained from the best fits, the mean cell numbers predicted by different *linear* models were comparable to the original model (Fig. 8.3a). Interestingly, the variance predicted by the original model was very high. For example, at day 8 the variance was 227-fold larger than the mean for $CM$ $CD8^+$ T cells, 50,456-fold larger than the mean for $EM$ $CD8^+$ T cells and 33,174-fold larger than the mean for $F$ $CD8^+$ T cells. This enormous variance matched the observed variation in the family sizes [5] and provided further support to the memory first linear model.

The variance predicted by different delayed differentiation *linear* models was comparable to the variance of the *linear basic* model (Fig. 8.3b). We compared the means and variances obtained from the 10,000 Gillespie simulations performed for all the *Branching* models with the *linear basic* model. Similar to the *linear* models, we found that the *Branching* models predict means and variances comparable to the *linear basic* model (Fig. 8.4). Thus, contrary to the Buchholz et al. [5] result using exponential models, we cannot discriminate between different linear and branching

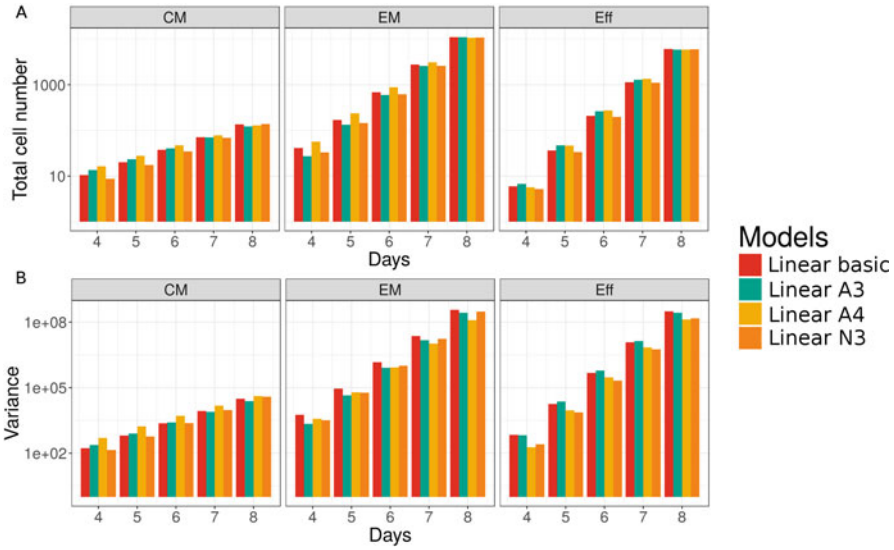


**Fig. 8.3** Comparison of means and variances predicted by various *linear* models. (**a**) The average cell numbers and (**b**) variance of central memory $CM$, effector memory $EM$ and effector $F$ CD8$^+$ T cells predicted for days 4 to 8 by the *linear basic*, *linear N3*, *linear A3* and *linear A4* models. For parameter values see Table 8.1

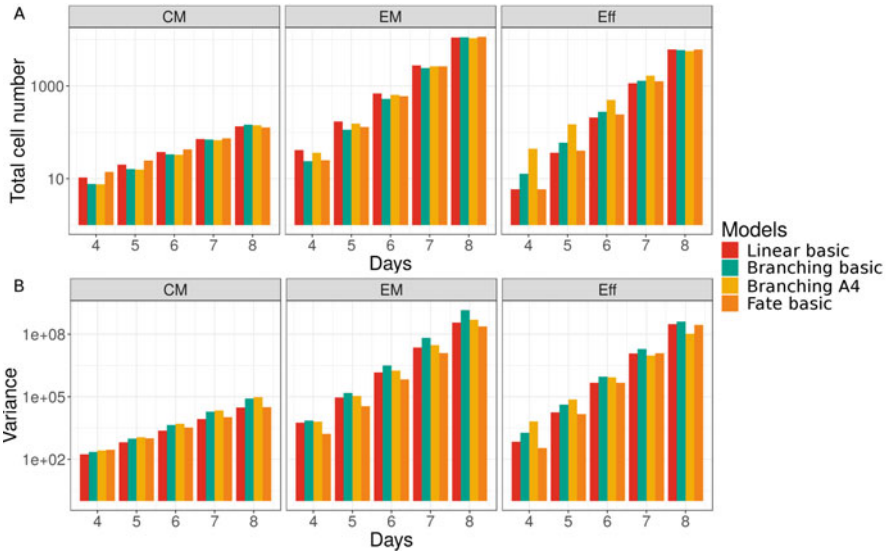


**Fig. 8.4** Comparison of means and variances predicted by various *Branching* and *Fate* models. (**a**) The average cell numbers and (**b**) variance of central memory $CM$, effector memory $EM$ and effector $F$ CD8+ T cells predicted for days 4 to 8 by the *linear basic*, *Branching basic* ($f = 0.5$), *Fate basic* ($f = 0.5$) and *Branching A4* ($f = 0.1$) models. For parameter values see Tables 8.2 and 8.3

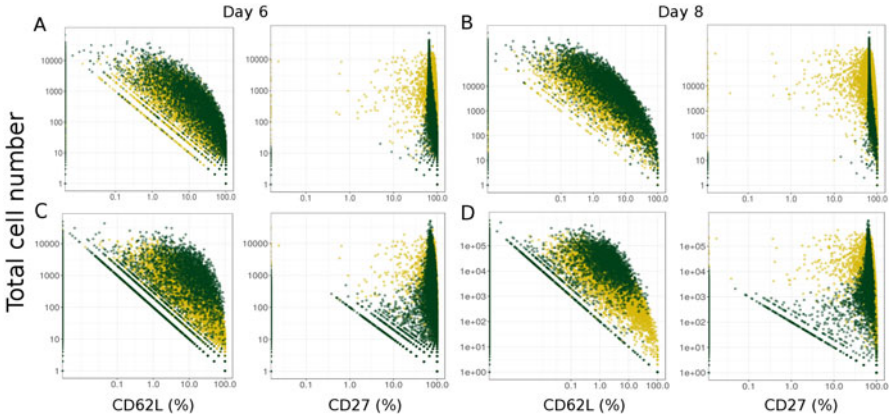


**Fig. 8.5** Different branching models exhibit variability in marker distribution. (**a**) Day 6 and (**b**) day 8 CD62L and CD27 marker distributions are plotted against family size distribution for the *Branching basic* model (green circles) and the *linear basic* model (yellow circles). (**c**) Day 6 and (**d**) day 8, the same CD62L and CD27 marker distributions for the *Branching A4* model (green circles) and *linear basic* model (yellow circles)

pathways using their predicted means and variances, when these pathways involve non-exponential differentiation steps.

In the single-cell tracing experiments of Buchholz et al. [5] and Gerlach et al. [4], the number of daughter cells produced by individual naïve $CD8^+$ T cell also exhibited wide heterogeneity in CD62L and CD27 marker distribution. Since $CM$ cells were defined as $CD62L^+CD27^+$ and $EM$ cells as $CD62L^-CD27^+$ [4, 5], we plotted the CD62L and CD27 marker distribution predicted by the *Branching* models and compared it to the marker distribution predicted by the original *linear basic* model. The *Branching basic* model predicted a CD62L marker distribution comparable to the *linear basic* model (Fig. 8.5a, b), i.e. a high variability in the number of $CD62L^+$ $CD8^+$ T cells per family size at day 6 and at day 8. The *Branching basic* model $CD8^+$ T cells exhibited a rather dichotomous distribution, i.e. most families are $CD27^+$ with very few cells being $CD27^-$ in them and most of the remaining families being typically $CD27^-$ with very few cells being $CD27^+$ in them (Fig. 8.5a, b). Thus, there were comparatively fewer families containing intermediate fraction of $CD27^+$ cells. Even though delayed differentiation in the *Branching* model resulted in comparable SSR values to the *Branching basic* model, we found that models like *Branching A4* predicted CD62L and CD27 marker variabilities that were comparable to the *linear basic* model (Fig. 8.5c, d). Overall we conclude that various models with non-exponential differentiation steps can predict similar population dynamics as the original model.

## 8.3 Conclusion

We used ordinary differential equation models to test how delays incorporated as transit compartments during cellular differentiation change the behaviour and prediction of different CD8$^+$ T cell differentiation models. Using a carefully designed set of single-cell tracing experiments, Buchholz et al. [5] showed that a linear differentiation model with progressive differentiation of naïve CD8$^+$ T cells to memory precursors to effector cells best fitted their data. Moreover, Buchholz et al. [5] showed that using variance and covariance of the data helps to choose between different models. However, Buchholz et al. [5] only considered models where cellular differentiation obeys a single exponential process. We show that allowing differentiation to be non-exponential can predict very similar dynamics and showed that a *Branching* model considering a non-linear pathway can have comparable population dynamics for the CD8$^+$ T cell subsets. We found that all models predicted comparable means and variances for the best fit parameter sets, making it difficult to distinguish between them. Comparing family sizes with marker distributions, we found that branching models that allow non-exponential differentiation perform better than the branching models that consider exponential functions for differentiation. Since allowing for non-exponential differentiation results in several models with comparable mean population dynamics and stochasticity, we think that further studies are required to identify the correct pathway of CD8$^+$ T cell differentiation.

## 8.4 Methods

We first generated data using the *linear basic* model using the parameters given in Buchholz et al. [5] (see Table 8.1). The models were fitted to the $log_{10}$ transformed total cell numbers obtained from the *linear basic* model. We used R package FME package with grind.R as a wrapper around FME to perform all the model fitting [19, 20]. Because the minimization of the sum of squared residuals (SSR) was not consistently achieved in iteration of the optimization gradient descent methods (like Nelder-Mead or quasi-Newton method like L-BFGS-B), we performed the minimization by first running a pseudorandom-search algorithm to achieve SSR values $\leq$ 0.5 (if possible) and then performed L-BFGS-B and Nelder-Mead iteratively until they converged on stable SSR values.

To perform Monte Carlo simulations using Gillespie algorithm, we used the StochKit2 software [21]. Different models were written in the form of kinetic equations, and 10,000 Gillespie instances were used for simulating CD8$^+$ T cell differentiation from day 0 to day 8. The means and variances were calculated using the 10,000 Gillespie simulations. Trajectories of individual naïve CD8$^+$ T cells and its progenies were used to compute marker heterogeneity and family sizes on days 6 and 8. The figures were plotted in MATLAB and R [22, 23].

**Acknowledgments** AP was financially supported by the European Union Seventh Framework Programme (FP7/2007–2013) under grant agreement 317040 (QuanTI) and by the Netherlands Organization for Scientific Research (NWO) VENI grant agreement 016.178.027.

## References

1. Stemberger C et al (2007) A single naive CD8 + T cell precursor can develop into diverse effector and memory subsets. Immunity 27:985–997
2. Blattman JN et al (2002) Estimating the precursor frequency of naive antigen-specific CD8 T cells. J Exp Med 195(5):657–664
3. Pewe LL et al (2004) Very diverse CD8 T cell clonotypic responses after virus infections. J Immunol 172(5):3151–3156
4. Gerlach C et al (2013) Heterogeneous differentiation patterns of individual CD8+ T cells. Science 340(6132):635–639
5. Buchholz VR et al (2013) Disparate individual fates compose robust CD8+ T cell immunity. Science 340(6132):630–635
6. Buchholz VR et al (2016) T cell fate at the single-cell level. Ann Rev Immunol 34:65–92
7. Gerlach C et al (2011) The descent of memory T cells. Ann N Y Acad Sci 1217(1):139–153
8. Pandit A, de Boer RJ (2019) Stochastic inheritance of division and death times determines the size and phenotype of CD8+ T cell families. Front Immunol 10:436
9. Chang JT et al (2007) Asymmetric T lymphocyte division in the initiation of adaptive immune responses. Science 315(5819):1687–1691
10. Schlub TE et al (2010) Predicting CD62L expression during the CD8+ T cell response in vivo. Immunol Cell Biol 88(2):157–164
11. Dowling MR et al (2014) Stretched cell cycle model for proliferating lymphocytes. Proc Natl Acad Sci 111(17):6377–6382
12. Duffy KR, Hodgkin PD (2012) Intracellular competition for fates in the immune system. Trends Cell Biol 22(9):457–464
13. Hawkins ED et al (2007) A model of immune regulation as a consequence of randomized lymphocyte division and death times. Proc Natl Acad Sci 104(12):5032–5037
14. Polonsky M et al (2016) Clonal expansion under the microscope: studying lymphocyte activation and differentiation using live-cell imaging. Immunol Cell Biol 94(3):242
15. Ganusov VV (2007) Discriminating between different pathways of memory CD8+ T cell differentiation. J Immunol 179(8):5006–5013
16. Gerritsen B, Pandit A (2016) The memory of a killer T cell: models of CD8+ T cell differentiation. Immunol Cell Biol 94(3):236–241
17. Gillespie DT (1977) Exact stochastic simulation of coupled chemical reactions. J Phys Chem 81:2340–2361
18. Gillespie DT (1992) A rigorous derivation of the chemical master equation. Phys A 188:404–425
19. Soetaert K, Petzoldt T (2010) Inverse modelling, sensitivity and Monte Carlo analysis in R using package FME. J Stat Softw 33(3):1–28
20. GRIND: http://theory.bio.uu.nl/rdb/grind.html
21. Sanft KR et al (2011) StochKit2: software for discrete stochastic simulation of biochemical systems with events. Bioinformatics 27(17):2457–2458
22. MATLAB R2016b (2016) The MathWorks, Inc., Natick
23. R Core Team R (2017) A language and environment for statistical computing. R Foundation for Statistical Computing, Vienna. https://www.R-project.org/